

See discussions, stats, and author profiles for this publication at: <https://www.researchgate.net/publication/45504034>

Phase Diagram of Hexahydro-1,3,5-trinitro-1,3,5-triazine Crystals at High Pressures and Temperatures

ARTICLE *in* THE JOURNAL OF PHYSICAL CHEMISTRY A · AUGUST 2010

Impact Factor: 2.69 · DOI: 10.1021/jp105226s · Source: PubMed

CITATIONS

39

READS

31

2 AUTHORS, INCLUDING:



Zbigniew Dreger

Washington State University

124 PUBLICATIONS 1,126 CITATIONS

SEE PROFILE

Phase Diagram of Hexahydro-1,3,5-trinitro-1,3,5-triazine Crystals at High Pressures and Temperatures

Zbigniew A. Dreger* and Yogendra M. Gupta

Institute for Shock Physics and Department of Physics, Washington State University,
Pullman, Washington 99164-2816

Received: June 7, 2010; Revised Manuscript Received: July 8, 2010

Raman spectroscopy and optical imaging were used to determine the phase boundaries between various hexahydro-1,3,5-trinitro-1,3,5-triazine (RDX) polymorphs. Experiments were performed on single crystals at pressures up to 8.0 GPa and temperatures ranging from room temperature to 550 K. Several distinct pressure regions were found in the RDX response at elevated temperatures: (i) melting of α -RDX followed by decomposition, below 2.0 GPa, (ii) decomposition of α -RDX between 2.0 and 2.8 GPa, (iii) irreversible transformation of α - and γ -RDX to ε -RDX between 2.8 and 6.0 GPa, and (iv) decomposition of γ -RDX above 6.0 GPa. A triple point between the α -, γ -, and ε -RDX was found at 3.7 GPa and 466 K. The α - γ phase transition was confirmed to occur at the same pressure, \sim 3.7 GPa, regardless of temperature, in the range of 295–460 K. Furthermore, it was determined that ε -RDX (i) has limited chemical stability under the pressure and temperature conditions where it is produced and (ii) decomposes according to the autocatalytic rate law. The findings reported here have provided new information about the response of RDX crystals at high pressures and temperatures.

1. Introduction

A good understanding of the phase diagram of high explosives (HE) at high pressures and temperatures is important for addressing performance and safety issues. In particular, detailed knowledge of polymorphism and structural and chemical stabilities is necessary to understand the reactive behavior of HE crystals over the range of pressures and temperatures relevant to shock wave initiation.

Here, we report on the phase diagram of single crystals of hexahydro-1,3,5-trinitro-1,3,5-triazine (RDX, $(\text{CH}_2\text{NNO}_2)_3$) at high pressures and temperatures. RDX, the cyclic trimer of methylenenitramine, is one of the most important crystalline energetic materials. It is widely used in explosives and monopropellants. Although extensively studied in recent years,^{1–11} the phase behavior and stability of RDX are not well established, especially at high pressure and temperature, where reactive behavior is of significant interest.

Recent studies have recognized that, depending on the external conditions, RDX can exist in several polymorphic phases: α , β , γ , δ , and ε . The α -polymorph is a stable form of RDX that exists at ambient conditions. The structure of this polymorph is well established; it is orthorhombic with $Pbca$ space group, and with eight molecules per unit cell.^{12,13} At pressures above \sim 3.8 GPa, α -RDX transforms into the γ -polymorph. This has been substantiated using X-ray diffraction^{10,14,15} and optical spectroscopy methods.^{1–6,8,16,17} This transformation has been observed under both static^{1–3,8,10,15–17} and shock-wave compression.^{4–6} It has also been established¹⁰ that the α - γ phase transition involves a decrease in unit cell volume of about 3% and leads to changes in the space group and molecular conformations. Specifically, the γ -RDX was found to have an orthorhombic structure of $Pca2_1$ space group, with eight molecules in the unit cell. Recent spectroscopic studies have

also suggested another high pressure form of RDX obtained at pressures above \sim 18 GPa, which has been tentatively termed as δ -RDX.⁹

RDX can also exist at ambient conditions in a metastable phase, labeled as β -RDX. This polymorph has been obtained either by crystallization from high boiling solvents^{11,12,18} or by deposition of RDX solution on a glass substrate.¹⁹ The structure of β -RDX has been determined recently¹¹ to be orthorhombic, with the same space group as γ -RDX but with different molecular conformations.

Using Raman¹⁶ and FTIR¹⁷ spectroscopy, it was shown that at high temperatures both the α - and the γ -RDX transform to the same high pressure–high temperature (HP–HT) polymorph. Based on some similarities in the vibrational spectra of the HP–HT polymorph and the β -polymorph, the authors of refs 16 and 17 concluded that the HP–HT polymorph is the β -RDX. However, very recent studies^{7,11} provided strong evidence that the HP–HT polymorph is not the same form as the β -RDX. Thus, the HP–HT polymorph was given a separate label as ε -RDX.^{7,11}

Although the studies presented in refs 16 and 17 provided phase diagrams for RDX polymorphs, the results from these two papers were largely inconsistent regarding the phase boundaries and the triple point. For example, the triple point locus differed by more than 100 K in the two studies (see Figure 1 for details). While these discrepancies are substantial, they have not been addressed to date. Experimental data are needed to address this inconsistency and provide an improved phase diagram for RDX.

The objective of this work was to determine the phase diagram of RDX, particularly regarding the boundaries between α -, γ -, and ε -RDX. Moreover, we wanted to obtain information on the stability and decomposition of the ε -polymorph. To address these objectives, we used Raman spectroscopy and optical imaging to distinguish between RDX phases. To mitigate problems typically encountered in high pressure studies of

* Corresponding author. E-mail: dreger@wsu.edu.

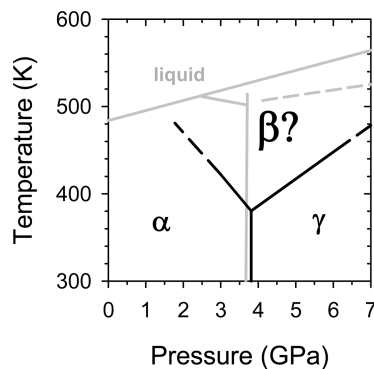


Figure 1. RDX phase diagrams based on data from refs 16 and 17. The HP-HT polymorph was inferred to be the β -RDX in these studies. Black lines are from ref 16 (dashed lines, extrapolation of experimental data). Gray lines are from ref 17 (dashed line, approximate phase boundary between γ - and HP-HT-polymorphs).

molecular solids (random sample morphology, grain interactions, and uncertain compression conditions), the present experiments were performed with good quality, single crystals under well-controlled pressure and temperature conditions.

The remainder of this Article is organized as follows. Experimental procedures, including high pressure and high temperature Raman measurements, are described briefly in the next section. Section 3 presents the experimental data and discussion regarding pressure–temperature (P – T) diagram, and chemical stability and decomposition kinetics of the ϵ -polymorph. The main findings of this work are summarized in section 4.

2. Experimental Method

Small, single-crystals (grains) of RDX were provided by Dr. D. E. Hooks of Los Alamos. The crystals were carefully selected on the basis of their quality and size. Using an optical microscope (160 \times), we selected crystals free of observable microscopic defects. Furthermore, the crystals selected had the appropriate dimensions to fill only a fraction of the high pressure cell compartment. Typically, the crystals did not exceed 0.12 mm on a side and 0.03 mm in thickness.

High pressure was generated in a modified Merrill–Bassett type diamond-anvil-cell (DAC). A stainless-steel gasket, pre-indented to 0.08 mm with a 0.2 mm hole drilled in the indentation, was used as a sample compartment. A single grain of RDX crystal and a ruby chip were loaded into the sample compartment, which was then filled with argon as a pressure-transmitting medium. The ruby fluorescence method utilizing R-line shifts was used to monitor pressure.²⁰ The precision of our pressure measurements at room temperature was estimated to be 0.05 GPa.

Temperature of the DAC was controlled using a resistive heater wrapped around the cell. The sample temperature was monitored with iron–constantan thermocouples. Two thermocouples were positioned on the facets of the diamond anvil, close to the diamond culet, and displaced from each other by about 180°. In the calibration experiments, the temperature in the cell compartment was calibrated by placing the head of an additional thermocouple into the gasket hole. The accuracy of the temperature measurements was determined to be ± 2 K.

The 532 line from a cw diode-pumped solid-state (DPSS) laser (Verdi-Coherent) was employed for Raman excitation. A Micro-Raman system (T64000, JY-Horiba) equipped with a microscope (Olympus BX-40) was used; it provided a spectral resolution of ~ 0.8 cm $^{-1}$ and a spatial resolution of 5 μ m.

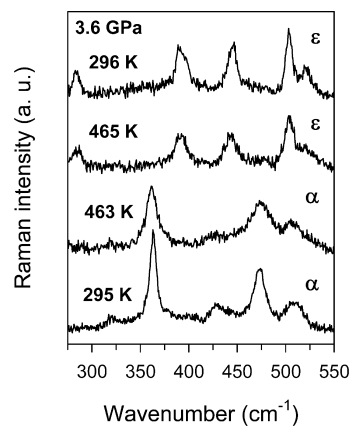


Figure 2. Raman spectra (300 – 600 cm $^{-1}$) of RDX single crystals at 3.6 GPa and several temperatures: 295 and 433 K (α -RDX), 465 and 296 K (ϵ -RDX). Raman spectra were acquired for 1 s and are offset vertically for clarity.

Experimental details regarding our Raman and ruby fluorescence measurement techniques can be found elsewhere.³ To avoid any irreversible effects of light on the sample, the exposure time and the laser irradiation power were kept at a low level. Specifically, the incident power on the sample did not exceed 50 mW, and the accumulation time of the Raman spectra was usually 1 s, and only occasionally 10 or 30 s.

To determine the pressure and temperature locus for the phase changes, the Raman measurements were performed at a specific pressure and with gradually increasing temperature. All experiments were carried out at pressures ranging from 0 to 8 GPa, and at temperatures ranging from ~ 295 to 550 K. Typically, for any given pressure, the RDX sample was slowly heated from room temperature at a rate of: 2–3 K/min up to ~ 423 K, 1–2 K/min from ~ 423 to ~ 473 K, and 1 K/min above ~ 473 K. The Raman spectra were acquired every 2 min from room temperature to ~ 473 K, and every 1 min above ~ 473 K. In studies of chemical stability and decomposition kinetics, both the pressure and the temperature remained unchanged to within ± 1 K over the duration of the experiment. At the same time, the Raman spectra and optical images were acquired alternately every ~ 30 s to determine the sample state.

3. Results and Discussion

3.1. P – T Diagram. To distinguish between RDX phases, the Raman spectra were measured at various frequency ranges. Two ranges, 300–600 cm $^{-1}$ (vibrations related to the triazine ring) and 2900–3100 cm $^{-1}$ (CH stretching vibrations), were found to be useful in the identification of RDX polymorphs. In Figures 2 and 3, we show typical spectra for the α - and γ -polymorphs, respectively, along with the spectral changes occurring at the transition to the ϵ -polymorph. Both transitions, α – ϵ and γ – ϵ , appeared within a minute of heating at the indicated temperatures. We found that the transitions were irreversible upon cooling, even down to room temperature. Thus, the ϵ -phase, once formed, could not be reverted to the α - or γ -phase by lowering the temperature. Furthermore, the ϵ -phase appeared to be stable over a broad pressure range at room temperature. Detailed information on the vibrational structure of the ϵ -polymorph can be found elsewhere.⁷

In Figure 4, we show the characteristic Raman spectra in the range of CH stretching modes obtained on the same sample. These spectra were acquired as follows: First, the sample was pressurized to 3.6 GPa and then heated. The spectrum was measured at the highest temperature in which the sample still

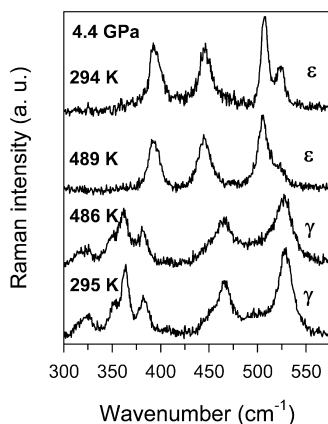


Figure 3. Raman spectra ($300\text{--}600\text{ cm}^{-1}$) of RDX crystals at 4.4 GPa and several temperatures: 295 and 486 K (γ -RDX), 489 and 294 K (ε -RDX). Raman spectra were acquired for 1 s and are offset vertically for clarity.

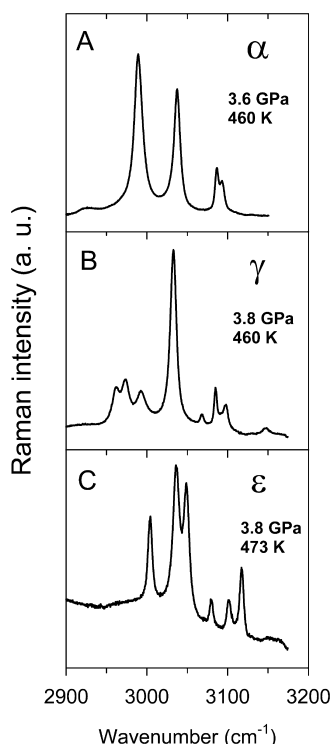


Figure 4. Raman spectra of CH stretching modes of RDX crystals measured near the triple point: (A) α -RDX (3.6 GPa, 460 K), (B) γ -RDX (3.8 GPa, 460 K), and (C) ε -RDX (3.8 GPa, 473 K). Raman spectra were acquired for 30 s.

remained in the α -phase (graph A). Next, the sample was transformed to the γ -phase by increasing the pressure to 3.8 GPa (graph B). Finally, the sample was heated to the transition temperature for the ε -phase (graph C). This experiment allowed us to locate the triple point between RDX phases, as being approximately at 3.7 GPa and 466 K.

Systematic measurements of the Raman spectra along with the optical images up to pressures of 8.0 GPa and temperatures of 550 K permitted determination of the boundaries between phases. The results from a series of experiments are presented in Figure 5. Symbols of various shapes denote the different RDX forms and phases obtained upon heating. The size of the symbols is larger than the maximum error in determining the particular event. Specifically, the temperature error of ± 5 K resulted from both the precision of the measurements and the effect of heating

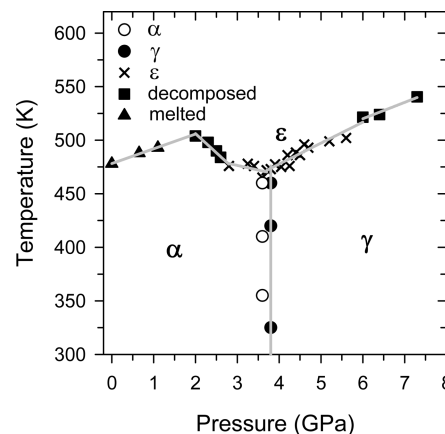


Figure 5. Phase diagram of RDX crystals as determined in the present work. Symbols of various types denote occurrence/existence of different RDX phases. Different phases determined using both Raman spectra and optical images. (○) α -RDX, (●) γ -RDX, (×) ε -RDX, (■) decomposed RDX, (▲) melted RDX. Gray lines are fits to each set of symbols.

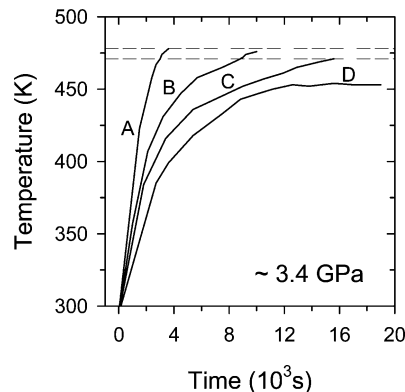


Figure 6. Effect of heating rate on the transition temperature of RDX from α to ε at ~ 3.4 GPa. Curves represent the measured temperature as a function of time. The transition occurred at the end of each curve: (A) transition at 478 K, (B) transition at 476 K, (C) transition at 471 K, and (D) no transition at 453 K within 5.5 h. Dashed lines denote the range of transition temperatures.

rate on transition temperatures. For example, as shown in Figure 6, the transition temperature from the α -polymorph to the HP-HT polymorph was somewhat dependent on the heating rate. For the case shown, when the heating rate was quadrupled, the temperature varied from 471 to 478 K. A number of sources can cause this variation, for example, reproducibility in the quality and size of the sample, reproducibility in temperature measurements (position of the thermocouple, thermal equilibration of the cell compartment), variation in pressure (± 0.1 GPa) among the three experiments, kinetically governed transition, etc. Because the overall differences in the temperatures were relatively small, it is believed that the observed temperature variations are caused by experimental reproducibility rather than the nature of the transition. Therefore, the transition to the ε -polymorph can be thought as being controlled mainly by thermodynamics instead of kinetics. For consistency in all our experiments, we used an intermediate heating rate similar to the one labeled "B" in Figure 6. Finally, pressure errors at elevated temperatures were estimated to be ± 0.1 GPa. Several distinct pressure regions have been observed in the behavior of RDX at elevated temperatures. Before we characterize these regions, it is worth mentioning that the α - γ phase transition occurred at the same pressure, about 3.7 GPa, regardless of temperature, in the range examined 295–460 K.

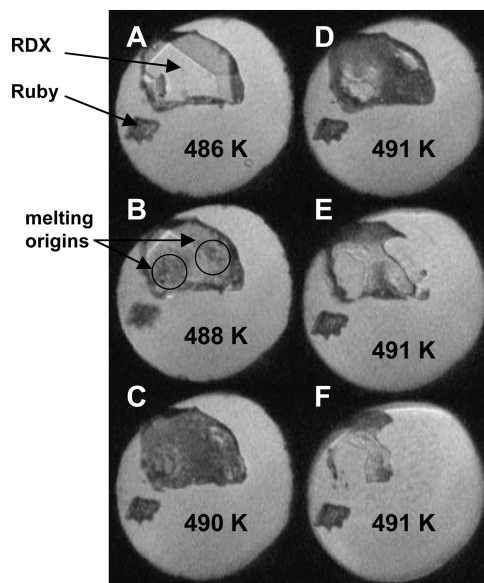


Figure 7. RDX crystal images at a pressure of 0.65 GPa and increasing temperatures. In all cases, only α -RDX was observed. (A) 486 K, no change in Raman spectra or optical images; (B) 488 K, melting initiated, origins of melting indicated by circles, $t = 0$; (C) 490 K, further melting but accompanied by decomposition, $t = 300$ s; (D) 490 K, further melting and decomposition, $t = 420$ s; (E) 491 K, further melting and decomposition, $t = 480$ s; and (F) 491 K, $t = 510$ s; the crystal almost disappears. Time was measured with respect to $t = 0$.

For pressures below 2.0 GPa, the heated RDX crystals showed melting rather than transformation to another solid phase. Melting was deduced from (i) a series of sample images clearly showing discolored spots (Figure 7) and (ii) a decrease in the intensity of the lattice modes. However, there were no new features in the intramolecular modes of the Raman spectra, which would be expected if another solid phase was formed. Also, it appeared that melting was followed by decomposition; this was corroborated by changes in the Raman spectra and optical images (see images B and C). In the case shown, at 0.65 GPa, the solid sample completely decomposed after ~ 500 s from the beginning of melting. The complete disappearance of a reacting material indicates the formation of gases that penetrated the liquid argon. Unfortunately, the reaction product could not be identified with Raman spectroscopy, likely because of insufficient volume and spatial distribution of the reacted species. Experiments with larger sample sizes will be needed for identifying the reaction products.

For pressures between 2.0 and 2.8 GPa, again, there was no indication of a transformation to another solid phase. However, in this instance, it appeared that the α -RDX was primarily decomposing (see images A–D in Figure 8a). The observed image changes were accompanied by a gradual decrease in Raman intensity. Ultimately, the Raman signal totally disappeared at the stage corresponding to image D. In contrast to the lower pressure range, the decomposed crystal remained intact in this pressure range. Further heating led to a transformation of the dark product into a brownish compound (see images E–H in Figure 8a). The compound appeared to be in a liquid phase due to its drop-like-shape. A successive cooling to room temperature and then a release of pressure indicated that the product was actually composed of liquid, solid, and gaseous phases (see images in Figure 8b). The molecular content of this compound could not be identified with reasonable confidence due to the strong background light in the Raman spectra that interfered with some new, weak bands.

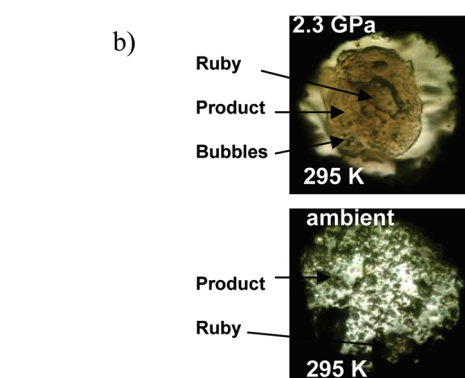
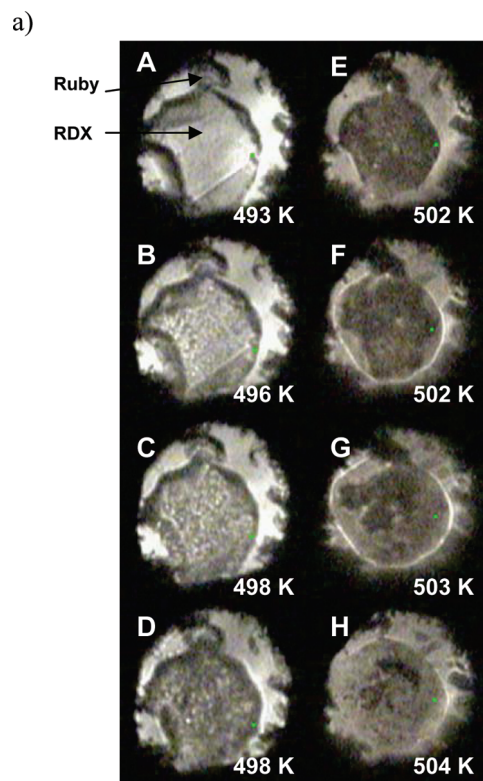


Figure 8. RDX crystal images at a pressure of 2.3 GPa and increasing temperatures. In all cases, only α -RDX was observed. (A) 493 K, no change; (B) 496 K, decomposition initiated, Raman signal decreases, no obvious melting seen, $t = 0$; (C) 498 K, progress in decomposition, $t = 180$ s; (D) 498 K, crystal decomposed, no Raman signal, $t = 300$ s; (E) 502 K, melting/disintegration of decomposed crystal observed, $t = 600$ s; (F) 502 K, further melting/disintegration, $t = 660$ s; (G) 503 K, further melting/disintegration, $t = 720$ s; and (H) 504 K, crystal almost completely melted/disintegrated, no Raman signal from this compound, $t = 840$ s. Time was measured with respect to $t = 0$.

For pressures between 2.8 and 6.0 GPa, the α - or the γ -polymorph was transformed to the ε -polymorph. Clear evidence of this was found in the Raman spectra, as indicated in Figures 2 and 3. Furthermore, as shown in Figure 9 (images A and B), the solid–solid phase transition does not affect the crystal quality, indicating that the transformation does not involve a large volume change.⁷ Further heating of the ε -polymorph led to its decomposition (C and D images), followed by transformation to a liquid (E and F images). It was surprising that the product obtained had much smaller volume than the crystal (compare the images E and F). However, consecutive cooling indicated that a fraction of the product was mixed with the pressure transmitting argon (see image H). We also point

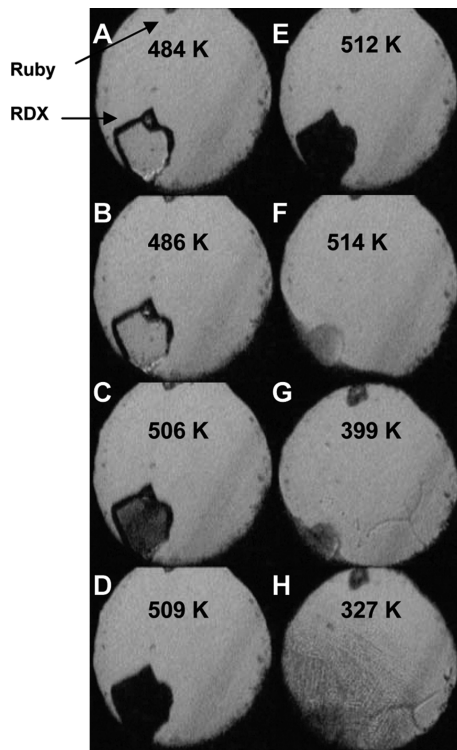


Figure 9. RDX crystal images at a pressure of 4.2 GPa and increasing temperatures. (A) 484 K, γ -RDX; (B) 486 K, ϵ -RDX, no change in the crystal quality; (C) 506 K, decomposition of crystal, $t = 0$ s; (D) 509 K, crystal decomposed, no Raman signal, $t = 480$ s; (E) 512 K, heating of decomposed crystal, $t = 780$ s; (F) 514 K, decomposed crystal melted/disintegrated, no Raman signal, $t = 900$ s; (G) 399 K, cooling of melted/disintegrated compound; and (H) 327 K, further cooling, no Raman signal from the melted/disintegrated compound. Time was measured with respect to $t = 0$.

out that once the Raman signal was lost, sample corresponding to image ‘‘D’’, it was not recovered in the course of further heating and cooling.

For pressures above 6.0 GPa, the heated γ -RDX underwent decomposition without transformation to ϵ -RDX. This behavior is similar to that in the pressure region of 2.0–2.8 GPa. In both cases, the decomposition pressure and temperature values are depicted by ‘■’ in Figure 5. It is clear from this study that decomposition above 2.0 GPa always left a solid residue, whereas the combination of melting and decomposition below 2.0 GPa did not.

The results presented here clearly differ from previously reported results.^{16,17} Although it is difficult to determine the source of these discrepancies, some remarks are in order. It is generally recognized that the effects of high pressure and temperature on molecular crystals can be affected significantly by experimental conditions. In particular, the experimental results can be influenced by the following: (i) sample morphology, polycrystals versus single crystals, (ii) nonhydrostaticity and pressure gradients, (iii) accuracy of temperature measurements and temperature gradients, (iv) interactions between the sample and pressure transmitting media, etc. Therefore, special care is required for obtaining reliable data with molecular solids under high pressures and temperatures.

3.2. Stability and Decomposition of ϵ -RDX. As shown in the previous section, the ϵ -polymorph appears to exist in a limited range of pressure and temperature from 2.8 to 6.0 GPa, and above ~ 465 K. Furthermore, it was found that this polymorph has limited stability at the pressure and temperature

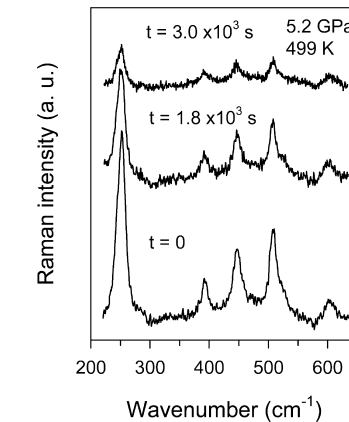


Figure 10. Selected Raman spectra of the ϵ -polymorph at 5.2 GPa and 499 K measured at different times. Background light was subtracted from the spectra. Spectra were acquired for 10 s and are offset vertically for clarity.

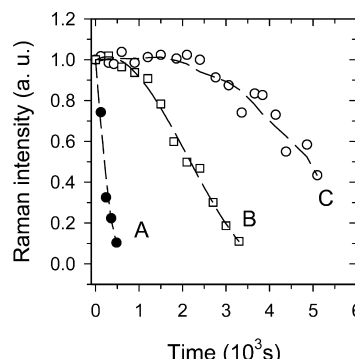


Figure 11. Normalized Raman intensity of the ϵ -polymorph as a function of time for selected pressures and temperatures: (A) 3.4 GPa, 499 K; (B) 5.2 GPa, 499 K; and (C) 3.4 GPa, 479 K. Dashed lines are drawn to guide the eye.

conditions where it is produced. Here, we present results regarding the decomposition kinetics of the ϵ -polymorph by utilizing the intensity changes in the Raman bands. Under unchanged experimental conditions such as excitation intensity, and excitation and collection geometry, Raman intensity can be related to the number/concentration of molecules of interest. In other words, a decrease in the intensity of the Raman bands could be indicative of a decreasing number of molecules, associated with the particular bands in the sample examined, and, therefore, can be the measure of the extent of decomposition. In Figure 10, we show typical spectra in the range of $200\text{--}650\text{ cm}^{-1}$ obtained at specific pressures and temperatures and different times. To acquire information on the changes in Raman intensity as decomposition proceeds, we followed changes in the intensity of five selected bands shown in Figure 10 and, in addition, a strong band at $\sim 900\text{ cm}^{-1}$ (not shown). The combined intensities from these six bands were averaged and then normalized to one at $t = 0$ (time equals zero). For decomposition at a given time, the intensity was normalized with respect to the value at $t = 0$.

In Figure 11, we present typical results of Raman intensity changes as a function of time, obtained at selected pressures and temperatures. In general, these curves reveal similar features: an initial plateau followed by an increasing slope, and, finally, at the end, a decreasing slope. The contributions of these characteristic features in the curves depend on the pressure–temperature values in the experiment. For example, curves A and C, obtained at 3.4 GPa and temperatures of 479 and 499 K, respectively, differ drastically in the length of the plateau. It

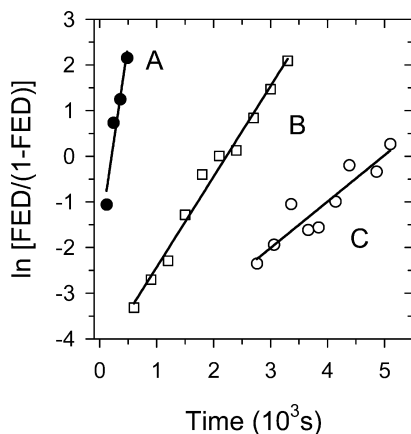


Figure 12. Plots of fractional extent of decomposition (FED) as a function of time for selected pressures and temperatures: (A) 3.4 GPa, 499 K; (B) 5.2 GPa, 499 K; and (C) 3.4 GPa, 479 K. Solid lines are from the least-squares fits to the experimental data. The rate constants obtained from the fits are in Table 1.

TABLE 1: Rate Constants of ϵ -RDX Decomposition at Several Pressures and Temperatures

pressure [GPa]	rate constants [10^{-3} s $^{-1}$]		
	479	487	499
3.4	1.0 ± 0.2	3.8 ± 0.5	8.5 ± 1.5
4.4			4.6 ± 0.3
5.2			2.1 ± 0.1

should be noted that curve “C” was obtained just above the boundary between the α -phase and ϵ -phase. It is clear that, in this case, the intensity did not change for a period of $\sim 2.4 \times 10^3$ s, indicating chemical stability of the ϵ -RDX at this time scale. In contrast, curve “A”, obtained at a temperature 20 °C higher than curve “C”, shows a decrease in intensity almost immediately after reaching decomposition temperature. Overall, a comparison of the curves in Figure 11 indicates that the stability of the ϵ -RDX in its pressure–temperature domain decreases with increasing temperature and decreasing pressure.

Because the decrease in Raman intensity can be related to the extent of decomposition, we can obtain the fractional extent of decomposition (FED) by subtracting the values in Figure 11 from unity. FED plots as a function of time are commonly used in determining the kinetics of thermal reactions, including the decomposition of solids.^{21,22} In particular, the sigmoid shape of the FED–time plots obtained indicates an autocatalytic-type reaction with three regions: induction, acceleration, and deceleration. A variety of autocatalytic rate equations in solid-state reactions have been derived to account for different mechanisms of reactions.²¹ As shown in Figure 12, our FED–time data can be fit to a relatively simple form of the autocatalytic rate equation:

$$\frac{d(\text{FED})}{dt} = k \times \text{FED} \times (1 - \text{FED}) \quad (1)$$

which on integration gives

$$\ln[\text{FED}/(1 - \text{FED})] = kt + C \quad (2)$$

where k is a global rate constant for decomposition.

Equation 2 is often identified with the Prout–Tompkins model, which was specifically formulated on the concept of

“nucleus branching”, which incorporates initiation, branching, and termination processes. Relation (2) can be obtained from the original Prout–Tompkins model by assuming a small nucleation rate.²¹ Although eq 2 is an oversimplification of a complex process governing solid-state decomposition, it permits a consistent extraction of the rate constant (k), even though the physical meaning of the rate is unclear. We also mention that eq 2 has already been utilized to study the thermal decomposition of HE, including HMX, RDX, and nitromethane.^{17,23}

The application of eq 2 to our data provides good fits (see Figure 12) and, therefore, can be used to evaluate the rate constants for ϵ -RDX decomposition at various temperatures and pressures (see Table 1). However, one should exercise caution regarding the absolute values of the obtained rates due to the limitations mentioned above. On the other hand, the pressure and temperature dependencies provide clear trends for ϵ -RDX decomposition in the studied P – T range, showing that: (i) at constant temperature (499 K), the rate of decomposition decreases with increasing pressure, and (ii) at constant pressure (3.4 GPa), the rate of decomposition increases with increasing temperature. Therefore, the activation volume for ϵ -RDX decomposition is found to be positive for these conditions, with decomposition governed by unimolecular processes. However, further studies are needed for more detailed information on these processes. This could be accomplished by monitoring the changes in the specific Raman modes related to the initial steps of decomposition, and by mapping out a broader range of pressures and temperatures.

4. Summary and Conclusions

Raman spectroscopy and optical imaging were used to examine the phase diagram of RDX single crystals up to 8.0 GPa and up to 550 K. The boundaries between three solid phases of RDX were determined under well-controlled experimental conditions. Our results show differences from previously reported results. The location of the triple point between the α -, γ -, and ϵ -RDX was evaluated to be at 3.7 GPa and 466 K. Several distinct pressure regions were observed for the RDX behavior at elevated temperatures. In particular, the transitions from α - and γ -RDX to the ϵ -RDX take place only in a narrow range of pressures (from 2.8 to 6.0 GPa) and temperatures (from 465 to 502 K). Below and above these pressures, α - or γ -RDX crystals decompose or melt instead of transforming to ϵ -RDX. Both the α – ϵ and the γ – ϵ transitions are irreversible at the phase boundaries, and the ϵ -phase could be quenched to room temperature. Also, it was confirmed that the α – γ phase transition occurred at the same pressure, about 3.7 GPa, regardless of temperature, over the temperature range 295–460 K. Chemical stability and decomposition of the ϵ -polymorph were examined in the pressure–temperature domain where it was produced. For this polymorph, it was determined that (i) chemical stability decreases at higher temperatures and lower pressures, (ii) decomposition obeys an autocatalytic rate law, and (iii) decomposition rates increase with increasing temperature and decreasing pressure. This study, on the P – T diagram of RDX single crystals, has provided new information on the behavior and properties of RDX at high pressures and temperatures; the P – T conditions considered here are relevant for understanding the RDX response to shock wave loading.

Acknowledgment. Dr. D. E. Hooks from Los Alamos is thanked for providing RDX crystals. This work was supported by ONR-MURI Grant N000149310369 and DOE Grant DEFG0397SF21388.

References and Notes

- (1) Goto, N.; Yamawaki, H.; Wakabayashi, K.; Nakayama, Y.; Yoshida, M.; Koshi, M. *Sci. Technol. Energ. Mater.* **2005**, *66*, 291.
(2) Goto, N.; Fujihisa, H.; Yamawaki, H.; Wakabayashi, K.; Nakayama, Y.; Yoshida, M.; Koshi, M. *J. Phys. Chem. B* **2006**, *110*, 23655.
(3) Dreger, Z. A.; Gupta, Y. M. *J. Phys. Chem. B* **2007**, *111*, 3893.
(4) Patterson, J. E.; Dreger, Z. A.; Gupta, Y. M. *J. Phys. Chem. B* **2007**, *111*, 10897.
(5) Dreger, Z. A.; Patterson, J. E.; Gupta, Y. M. *J. Phys.: Conf. Ser.* **2008**, *121*, 04201.
(6) Patterson, J. E.; Dreger, Z. A.; Miao, M.; Gupta, Y. M. *J. Phys. Chem. A* **2008**, *112*, 7374.
(7) Dreger, Z. A.; Gupta, Y. M. *J. Phys. Chem. A* **2010**, *114*, 7038.
(8) Cieza, J. A.; Jenkins, T. A.; Liu, Z.; Hemley, R. J. *J. Phys. Chem. A* **2007**, *111*, 59.
(9) Cieza, J. A.; Jenkins, T. A. *Propellants, Explos., Pyrotech.* **2008**, *33*, 390.
(10) Davidson, A. J.; Oswald, I. D. H.; Francis, D. J.; Lennie, A. R.; Marshall, W. G.; Millar, D. I. A.; Pulham, C. R.; Warren, J. E.; Cumming, A. S. *CrystEngComm* **2008**, *10*, 162.
(11) Millar, D. I.; Oswald, I. D. H.; Francis, D. J.; Marshall, W. G.; Pulham, C. R.; Warren, J. E.; Cumming, A. S. *Chem. Commun.* **2009**, 562.
(12) McCrone, W. C. *Anal. Chem.* **1950**, *22*, 954.
(13) Choi, C. S.; Prince, E. *Acta Crystallogr., Sect. B* **1972**, *28*, 2857.
(14) Olinger, B.; Roof, B.; Cady, H. *Proceedings of International Symposium on High Dynamic Pressures*; Paris, France, 1978; p 3.
(15) Yoo, C. S.; Cynn, H.; Howard, W. M.; Holmes, N. *Proceedings of the 11th International Detonation Symposium, Snowmass*; U.S., 1998; p 951.
(16) Baer, B. J.; Oxley, J.; Nicol, M. *High Pressure Res.* **1990**, *2*, 99.
(17) Miller, P. J.; Block, S.; Piermarini, G. J. *Combust. Flame* **1991**, *83*, 174.
(18) Karpowicz, R. J.; Sergio, S. T.; Brill, T. B. *Ind. Eng. Chem. Prod. Res. Dev.* **1983**, *22*, 363.
(19) Torres, P.; Mercado, L.; Cotte, I.; Hernandez, S. P.; Mina, N.; Santana, A.; Chamberlain, R. T.; Lareau, R.; Castro, M. E. *J. Phys. Chem. B* **2004**, *108*, 8799.
(20) Barnett, J. D.; Block, S.; Piermarini, G. J. *Rev. Sci. Instrum.* **1973**, *44*, 1.
(21) Brown, W. E.; Dollimore, D.; Galwey, A. In *Reactions in the Solid State, Comprehensive Chemical Kinetics*; Bamford, C. H., Tipper, C. F. H., Eds.; Elsevier: Amsterdam, 1980.
(22) Brown, M. E. *Thermochim. Acta* **1997**, *300*, 93.
(23) Piermarini, G. J.; Block, S.; Miller, P. J. *J. Phys. Chem.* **1987**, *91*, 3872; **1989**, *93*, 457.

JP105226S